Oil Shale, 2024, Vol. 41, No. 2, pp. 103–114
doi: https://doi.org/10.3176/oil.2024.2.02
ISSN 0208-189X

Geochemical and thermal characterization and kinetics of oil shale samples from Çeltek, Türkiye

Mustafa Verşan Kök*

Department of Petroleum and Natural Gas Engineering, Middle East Technical University, Dumlupınar Blv. 1, 06800 Ankara, Türkiye

Received 4 January 2024, accepted 19 April 2024, available online 30 April 2024

Abstract. *This research delves into the geochemical aspects, non-isothermal thermogravimetric analysis, and model-free kinetics of oil shale samples from the Çeltek region in Amasya, Türkiye. Shifting the focus to the core of the research, thermal and mass spectrometric analysis (TG–DTG–MS) experiments were conducted in an air atmosphere, employing three distinct heating rates of 10, 20, and 30 °C/min. The outcomes revealed two successive reaction stages: the breakdown of organic matter and mineral decomposition. In the breakdown stage, activation energy values exhibited a range of 160–163 kJ/mol, while in the mineral decomposition stage, the values varied between 208–214 kJ/mol, using model-free kinetic models.*

Keywords: *oil shale, geochemical analysis, mass spectrometry, thermogravimetry, thermal analysis, model-free kinetics.*

1. Introduction

Oil shale, a finely-grained sedimentary rock, contains an organic component known as kerogen. When oil shale is heated to high temperatures in a process called pyrolysis or retorting, kerogen is converted into oil, gas, and other by-products. This process is distinct from combustion, where the primary outcome is the release of heat energy. Combustion of oil shale produces by-products such as carbon dioxide, water vapor, and various pollutants, depending on combustion conditions and the composition of oil shale [1].

Typically embedded in sedimentary rocks, oil shale comprises clay minerals (kaolinite, smectite, illite, and chlorite), carbonate minerals (calcite and dolomite), and diverse minerals, such as quartz, feldspar and pyrite, alongside organic matter. In Türkiye, primary oil shale deposits from the Paleocene–Eocene and Middle–Upper Miocene ages represent the country's

* Corresponding author, kok@metu.edu.tr

second-largest fossil fuel reservoir, following coal and lignite deposits. Key oil shale deposits, namely Beypazarı, Seyitömer, Himmetoğlu, and Hatıldağ, concentrated in the middle and western Anatolian regions, boast proven open-cast explored reserves of approximately 470 million tons [2].

Various thermal analysis techniques, such as differential scanning calorimetry (DSC), thermogravimetry (TGA), and thermogravimetric analysis–mass spectrometry (TGA–MS), are extensively employed to assess the combustion properties and kinetics of oil shale samples under diverse process conditions [3–8]. Additionally, researchers combine Fisher assay and Rock-Eval techniques with TGA–MS to measure the oil yields of oil shale samples [9–12], offering crucial insights into oil shale conversion potential via various recovery methods.

This research on the Çeltek oil shale deposit goes beyond conventional approaches, incorporating simultaneous TGA–MS and utilizing diverse geochemical and organic techniques – pyrolysis, total organic carbon (TOC) analysis, gas chromatography (GC), and gas chromatography–mass spectrometry (GC–MS) – for comprehensive characterization. Remarkably, this research marks the first detailed thermal analysis and kinetic study of Çeltek oil shale in the oil shale literature, contributing significantly to our understanding of the properties of Çeltek oil shale and its potential for development through distinct recovery techniques.

2. Experimental materials and methods

This study investigates oil shale samples from the Çeltek region, specifically targeting the oil shale layer within the coal and bituminous shale occurrences of the Çeltek Formation. The research aims to discern the geochemical, thermal, and kinetic properties of these samples. To facilitate the experiments, raw oil shale samples underwent grinding, mixing, and homogenization processes. Approximately 10 mg of the resulting samples, with a particle size of <60 mesh, were meticulously prepared following ASTM D2013-72 guidelines.

Thermal analysis experiments were conducted over a temperature range of 25–900 °C, employing three distinct heating rates (10, 20, and 30 °C/min). Each experiment utilized approximately 10 mg of oil shale to mitigate the impact of temperature distribution within the sample, while maintaining a constant flow rate through the sample pan at 50 mL/min.

Before the commencement of experiments, thorough balance and temperature calibrations were conducted for the thermal analysis systems. To ensure the reliability of the results, all experiments were carried out twice, demonstrating a high level of consistency in repeatability experiments, with a standard error of ±1–2 °C. This rigorous approach to sample preparation and experimental procedures enhanced the reliability and robustness of the obtained geochemical, thermal, and kinetic data for the oil shale samples from Çeltek.

3. Results and discussion

Investigations into Türkiye's oil shale deposits carry significant implications for the country's long-term energy demand projections and strategic planning. This study examines explicitly the geochemical, organic, and thermal characteristics of the Middle–Upper Eocene bituminous sediments within the Çeltek Formation in the Suluova and Çorum basins, situated in the Sakarya Tectonic Zone (Figure 1).

The Suluova and Çorum basins play a crucial role in petroleum research due to the presence of hydrocarbon gas accumulations in Eocene sedimentary rocks, particularly within the Çeltek Formation. Furthermore, noteworthy traces of asphalt have been identified in rock outcrops in these regions [14]. Bearing oil shale and coal deposits, the Çeltek Formation unconformably overlies the basement rocks of the Jurassic–Cretaceous age. The succession begins with a conglomerate at the bottom, followed by layers of sandstone, claystone, and siltstone, interspersed with oil shale and coal deposits, all seamlessly transitioning from one to the other. Oil shales exhibit thicknesses varying from 5 to 10 meters. Situated just above coal deposits in the region, the silicified limestone has an average thickness of 0.3 meters.

The Çeltek oil shale predominantly contains micro-layered clay-rich and humic-rich layers. The humic-rich layers are comprised of vitrinite (35–45%), liptinite (5–9%), and inertinite (3–5%). The huminitic organic matter in the oil shale is mainly composed of gelinite. The reflectance values of vitrinite in the oil shale samples range between 0.23 and 0.52% R_{max}. The maceral composition of the studied samples shows that oil shale is amosite. The TOC values of the oil shale range from 1.23% to 7.15%. While the bituminous shales studied in the Çeltek Formation exhibit calorific values up to 1400 kcal/kg, their average field value is 600 kcal/kg. The Amasya-Çeltek field has probably up to 90 million tons of oil shale reserves [15, 16].

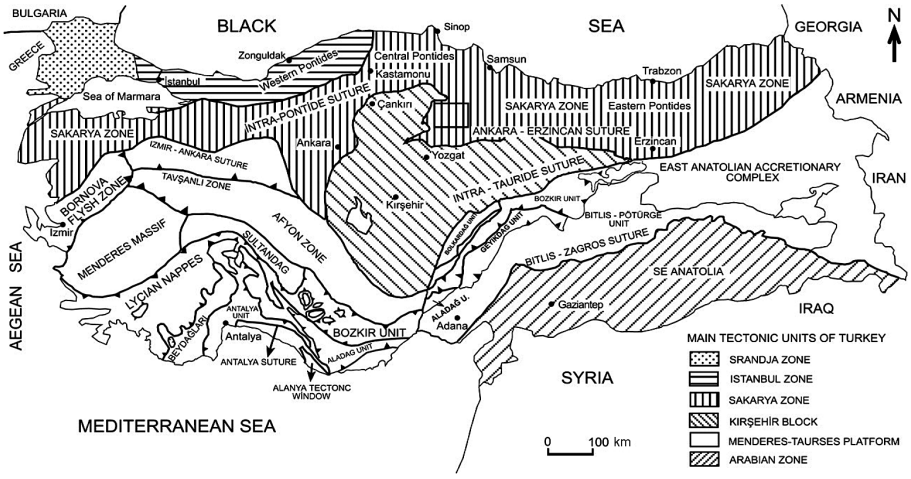

Fig. 1. Principal tectonic units in Türkiye [13].

3.1. Source of organic matter input and paleo-depositional conditions

The first part of this investigation delves into the outcomes derived from GC, isotope analysis, and GC–MS techniques [17]. The distribution of normal alkanes, coupled with relatively high carbon preference index (CPI) values, signifies the incorporation of mixed organic matter in both studied samples, Çeltek-1 and Çeltek-2, notably featuring substantial inputs of terrigenous organic matter during depositions. The examined samples exhibit normal alkanes within the C_{16}–C_{34} range, yielding CPI values ranging from 1.35 to 1.45 and from 1.20 to 1.35, respectively. This observation is further supported by the analysis of isoprenoids and their ratios, such as Pr/Ph, Pr/n-C_{17}, and Ph/n-C_{18} (Table 1).

Table 1. Gas chromatography and Rock-Eval analysis results of oil shale samples [17]

Oil shale	Pr/Ph	Pr/n-C_{17}	Ph/n-C_{18}	$CPI_{16–32}$	$CPI_{24–34}$	$^{13}C_{Sat}$	$^{13}C_{Bulk}$	$^{13}C_{Aro}$
Çeltek-1	1.67	28.00	10.50	1.35	1.20	–33.80	–33.75	–32.93
Çeltek-2	2.55	4.48	2.90	1.40	1.35	–31.12	–29.85	–29.65
	TOC	**S_2**	**S_3**	**T_{max}**	**HI**	**OI**	**PI**	**RC/PC**
Çeltek-1	3.93	29.17	1.64	437	742	42	0.01	1.4/2.5
Çeltek-2	3.19	25.55	0.28	440	801	9	0.01	1.0/2.18

S_2 – amount of hydrocarbons generated through thermal cracking of nonvolatile organic matter, S_3 – amount of CO_2 (in mg of CO_2 per g of rock) produced during pyrolysis of kerogen, HI – hydrogen index, OI – oxygen index, PI – production index, RC – residual carbon, PC – pyrolysis carbon

Based on the analysis results presented in Table 1, the studied samples were deposited under sub-oxic to relatively oxic environmental conditions. Specifically, the Çeltek-2 sample indicates deposition under highly oxic environmental conditions, as reflected in its Pr/Ph ratio of 2.55. On the other hand, the bulk stable ^{13}C of the shale samples further supports the assessment of contributions from terrigenous organic matter. The ^{13}C compositions of the saturated and aromatic fractions exhibit values ranging from –33.80% to –31.12% and from –32.93% to –29.65%, respectively.

3.2. Rock-Eval analysis

The assessment of organic matter in the examined oil shale samples was conducted using TOC content and Rock-Eval pyrolysis data. TOC is a crucial indicator for the quantities of kerogen and bitumen in the source rock, representing the combined carbon content of the kerogen and the hydrocarbons derived from it, which remain within the rock.

This study revealed that the TOC content in the oil shale samples fell within the range of 3.19% to 3.93% by weight. According to the TOC classification criteria, the Çeltek oil shale samples can be categorized as deemed minimum or cut-off TOC content for oil shales. Conversely, the Rock-Eval analysis results (Table 1) indicate that the oil shale samples exhibit a moderate to good source rock potential, aligning with type I kerogen. Generally, higher hydrogen contents in kerogen indicate a more substantial oil-generating potential. The temperature at which the maximum quantity of organic S_2 hydrocarbons is produced, known as T_{max}, serves as a rudimentary measure of the thermal maturity of organic matter, influenced by the type of organic matter. Additionally, the amount of petroleum generated and expelled from the source rock tends to increase with the rise in the atomic hydrogen index of the organic matter [18–20].

3.3. Thermogravimetric analysis of oil shale samples

The examination of oil shale pyrolysis through TG–MS applications revealed the intricacies of a multi-stage process. The temperature profiles and derivative mass loss curves of the oil shale samples, subjected to three constant heating rates, are illustrated in Figure 2. Distinct stages in the combustion process are evident in the derivative curves. Before the pyrolysis stage, moisture release corresponding to the liberation of water vapor from the mineral layer was observed during preheating the samples at approximately 275 °C. Subsequently, in the pyrolysis stage, where the temperature reached up to 600 °C, various volatile organic compounds, including shale oil, gases (methane, ethane, propane, and hydrogen), and char (carbonaceous residue), were released, signifying the breakdown of organic matter.

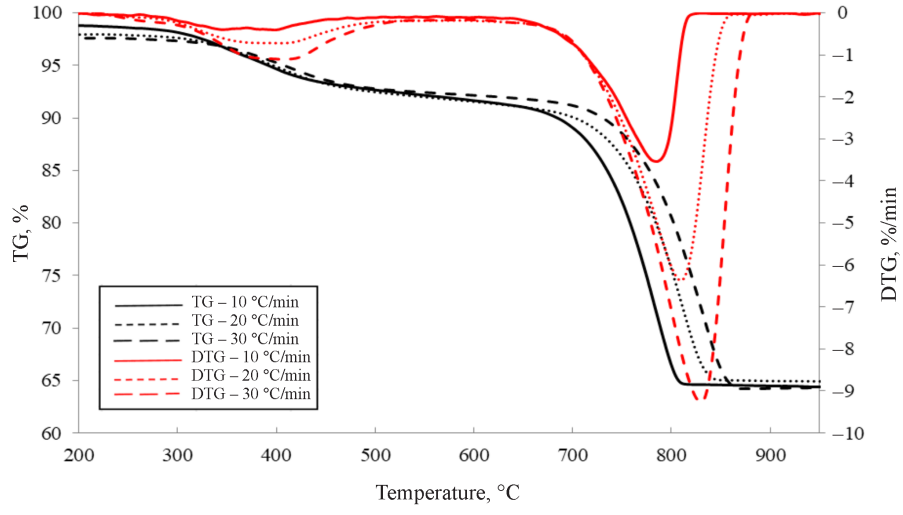

Fig. 2. TG-DTG curves of Çeltek oil shale at different heating rates.

The second stage involved upgrading the products obtained from pyrolysis to more valuable hydrocarbons, inducing the decomposition of mineral matter within the range of 670–780 °C. This may include refining shale oil into transportation fuels (gasoline, diesel, and jet fuel) through processes such as hydrotreating, hydrocracking, and distillation. Additionally, gases produced during pyrolysis can be further processed and purified for use as fuel or feedstock in various industrial applications. The first stage exhibited a mass loss of 1.2–4.6%, while the second stage demonstrated a mass loss ranging from 11.2% to 58.2%, contingent upon the heating rate. The 3% average mass loss in the first stage resulted from the thermal decomposition of kerogen, forming oil shale. Conversely, the 35% average mass loss in the second stage primarily arose from the thermal decomposition of various minerals in the oil shale samples.

The analysis of thermogravimetric data involved calculating critical parameters, such as reaction regions, mass loss, derivative mass loss, ignition, peak and burn-out temperatures, ignition, combustion, as well as reactivity, ignition and combustion indexes for the oil shale samples at each heating rate (Table 2). In general, reactivity elucidates the combustion characteristics of oil shale samples at a specific conversion rate. Conversely, ignition and combustion indexes provide insights into the stability of oil shale combustion under varying conditions.

The following equations were utilized to ascertain the combustion index and reactivity, respectively [21–23]:

$$S = R_{max} \times R_a / T_i^2 \times T_b, \tag{1}$$

$$R = (-1/W_o) \times (dW/dt), \tag{2}$$

where R_{max} is the maximum combustion rate, R_a is the average mass loss rate, W_o is the initial mass of the sample, dW/dt is the maximum rate of mass loss, T_i is the ignition temperature, and T_b is the burn-out temperature.

Remarkably, increased reactivity, ignition and combustion index values with a rise in the heating rate indicated enhanced combustion characteristics. Furthermore, the thermogravimetric data underscored that the reaction intervals and corresponding peak and burn-out temperatures increased in each reaction stage, as the heating rate was elevated.

Table 2. Thermogravimetric analysis of Çeltek oil shale samples

Properties Çeltek-1 Çeltek-2	**10 °C/min**	**20 °C/min**	**30 °C/min**
Reaction intervals, 1st stage	240–558 243–560	244–566 248–569	256–590 261–573
Peak temperature, °C	382 384	391 390	402 398
Reaction intervals, 2nd stage	558–834 554–838	566–868 561–871	590–882 584–885
Peak temperature, °C	785 782	810 813	829 826
Ignition temperature, °C	67 71	34 38	22 24
Burn-out temperature, °C	834 838	868 871	882 885
Peak time, min	74 76	38 37	26 24
Burn-out time, min	79 81	41 38	28 27
Mean mass loss, %/min	0.426 0.425	0.788 0.775	1.185 1.103
Maximum mass loss, %/min	3.531 3.642	6.368 6.376	9.271 8.784
Ignition index, $\%/min^{-3}$	0.70 0.73	4.90 3.98	15.68 14.87
Combustion index, 10^{-8} $wt\%^2/min^2\,C^3$	0.356 0.320	1.143 1.126	2.466 2.346
Reactivity, $wt\%^2/mg\ min$	0.31 0.30	0.32 0.33	0.35 0.37

3.4. Mass spectrometric analysis

In mass spectrometric analysis, the signal intensity of the iron current serves as an indicator of the concentration of gaseous components at varying temperatures. Concurrent TG–MS applications enable to assess whether diverse compounds present in the product are being formed simultaneously.

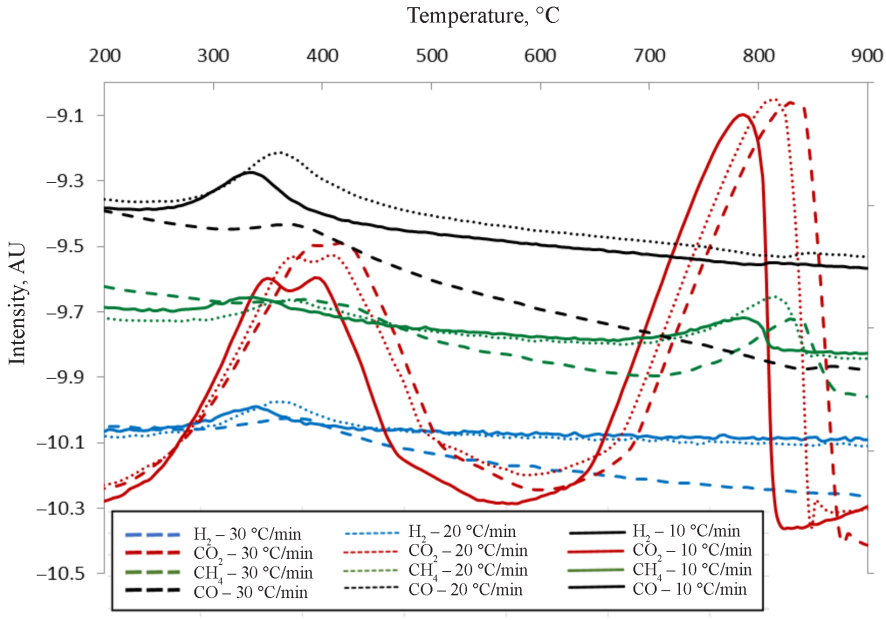

Fig. 3. MS curves of Çeltek oil shale samples at different heating rates.

The signal intensity is utilized as an approximate quantification method to compare the compositions of distinct compounds [24].

The analysis of Çeltek oil shale samples with the mass spectrometer focused on monitoring various gaseous species (Fig. 3). During the initial stage involving the breakdown of organic matter within the temperature range of 244–590 °C, the thermal decomposition of kerogen predominantly led to the production of carbon dioxide (CO_2) and methane (CH_4). Additionally, carbon monoxide (CO) was generated during this phase. In the subsequent stage, the decomposition of mineral matter within the temperature range of 558–882 °C, various minerals underwent decomposition, resulting primarily in the formation of CO_2 and CH_4.

3.5. Kinetic analysis

The determination of oil shale kinetics commonly employs non-isothermal model-free methods due to the presence of organic material (kerogen) in oil shale samples. The thermal decomposition of kerogen unfolds in successive stages, where, in the initial stage, kerogen decomposes into bitumen and gas. Subsequently, in the successive stage, bitumen decomposes into oil, gas, and char [25].

For the kinetic analysis of oil shale samples, two distinct model-free kinetic methods, KAS (Kissinger–Akahira–Sunose) and OFW (Ozawa–Flynn–Wall), were employed to determine the activation energy – the minimum energy

required for chemical reactions, directly proportional to the amount of heat absorption [26, 27]. Model-free methods allow the calculation of kinetic properties at progressive conversion degrees; therefore, a series of experiments were performed at different heating rates, and then, the temperature values at fixed conversion degrees were measured for each heating rate.

The final form of OFW is given below, where activation energy is obtained from the slope of ln β vs. $1/T$ plot for each conversion degree [28–33]:

$$\ln \beta = \ln[AE/R\, g(\alpha)] - 5.331 - 1.052\ (E/RT), \tag{3}$$

where α is the amount of samples undergoing a reaction, E is the activation energy, β is the heating rate, T is the peak temperature, R is the gas constant, and A is the Arrhenius constant.

The KAS method, on the other hand, uses the following expression, where activation energy is obtained from the slope of $\ln(\beta/T^2)$ vs. $1/T$ plot for each conversion degree:

$$\ln(\beta/T^2) = \ln[AE/E\, g(\alpha)] - E/RT. \tag{4}$$

Applying both kinetic methods, a linear relationship (correlation coefficients were between 0.97 and 0.99) was observed at each conversion degree. Finally, the activation energy values were calculated from the corresponding slopes at each conversion level according to the OFW and KAS models.

The calculated activation energy values for Çeltek oil shale samples at each conversion degree (ranging from 0.1 to 0.9) are presented in Table 3. Notably, the activation energy values for the organic matter breakdown stage ranged from 158 to 163 kJ/mol. In contrast, for the mineral matter decomposition stage, the values ranged from 208 to 214 kJ/mol. It can be concluded that the results presented in this research align with those of other similar published research articles.

Table 3. Activation energy (kJ/mol) of Çeltek oil shale samples

Conversion degree, α	**OFW, 1st stage** Çeltek-1 Çeltek-2	**KAS, 1st stage** Çeltek-1 Çeltek-2	**OFW, 2nd stage** Çeltek-1 Çeltek-2	**KAS, 2nd stage** Çeltek-1 Çeltek-2
0.1	133 129	130 127	203 206	198 202
0.2	122 124	118 116	215 218	210 213
0.3	119 114	115 116	217 213	212 215

Table 3 (continued)

0.4	127 122	123 119	217 213	211 214
0.5	143 138	139 133	217 216	210 205
0.6	154 146	151 149	216 214	210 211
0.7	180 174	178 171	215 211	208 209
0.8	239 241	240 243	218 220	212 214
0.9	251 246	254 248	210 205	205 206
E (kJ/mol)	**163** **159**	**160** **158**	**214** **213**	**208** **210**

4. Conclusions

This study presents a comprehensive characterization of Çeltek oil shale samples, with a specific focus on geochemical, thermal, and kinetic aspects. The thermal and kinetic analyses were conducted using simultaneous thermogravimetry–mass spectrometry, employing three different heating rates.

1. Two discernible stages were identified during the simultaneous TG–MS experiments: the breakdown of organic matter and the decomposition of mineral matter regions. Notably, these stages provided insights into the intricate thermal behavior of the oil shale samples.
2. As the heating rate increased, the thermal properties of the oil shale samples – reactivity, ignition and combustion indexes, reaction intervals, peak temperatures, and burn-out temperatures – all showed an upward trend. This finding highlights the significant impact of the heating rate on the thermal behavior of the oil shale samples.
3. Minimal variation was noted in determining activation energy values based on the applied kinetic methods and model assumptions. This consistency suggests robustness in the derived activation energy values across different approaches, emphasizing the reliability of the kinetic analyses employed in this research.

Acknowledgments

The author sincerely thanks both reviewers for their abundant critical and constructive comments. The publication costs of this article were covered by the Estonian Academy of Sciences.

REFERENCES

1. Oja, V., Suuberg, E. M. Oil shale processing, chemistry, and technology. In: *Fossil Energy*. Springer, New York, 2013, 99–148.
2. Şener, M., Şengüler, İ ., Kok, M. V. Geological considerations for the economic evaluation of oil shale deposits in Turkey. *Fuel*, 1995, **74**(7), 999–1003.
3. Williams, P. T., Ahmad, N. Influence of process conditions on the pyrolysis of Pakistani oil shales. *Fuel*, 1999, **78**(6), 653–662.
4. Al-Harahsheh, M., Al-Ayed, O. Effect of demineralization and heating rate on the pyrolysis kinetics of Jordanian oil shale. *Fuel Proc. Technol*., 2001, **92**(9), 1805–1811.
5. Kök, M. V., Pamir, M. R. Pyrolysis kinetics of oil shales determined by DSC and TG/DTG. *Oil Shale*, 2003, **20**(1), 57–68.
6. Kök, M. V., Pamir, M. R. Comparative pyrolysis and combustion kinetics of oil shales. *J. Anal. Appl. Pyrol*., 2000, **55**(2), 185–194.
7. Shawabkeh, A., Abdel Halim, K. S., Al-Ayed, O. 2016. Isoconversional methods for kinetic modeling of kerogen pyrolysis using TG data. *Appl. Mech. Mater*., 2016, **835**, 299–307.
8. Kök, M. V., Iscan, A. G. Oil shale kinetics by differential methods. *J. Therm. Anal. Calorim.*, 2007, **88**, 657–661.
9. Kaljuvee, T., Keelmann, M., Trikkel, A., Kuusik, R. Thermo-oxidative decomposition of oil shales. *J. Therm. Anal. Calorim.*, 2011, **105**, 395–403.
10. Kaljuvee, T., Pelt, J., Radin, M. TG-FTIR study of gaseous compounds evolved at thermooxidation of oil shale. *J. Therm. Anal. Calorim.*, 2004, **78**, 399–414.
11. Li, S., Yue, C. Study of different kinetic models for oil shale pyrolysis. *Fuel Proc. Technol.*, 2004, **85**(1), 51–61.
12. Li, S., Yue, C. Study of pyrolysis kinetics of oil shale. *Fuel*, 2003, **82**(3), 337–342.
13. Gorur, N., Tuysuz, O. Cretaceous to Miocene palaeographic evolution of Turkey: implications for hydrocarbon potential. *J. Petrol. Geol.*, 2007, **24**(2), 119–146.
14. Görür, N., Oktay, F. Y., Seymen, I., Şengör, A. M. C. Palaeotectonic evolution of the Tuzgölü basin complex, central Turkey: sedimentary record of a Neo-Tethyan closure. *Geological Society*, 1984, **17**, 467–482.
15. Şener, M., Şengüler, İ. Geological, mineralogical, and geochemical characteristics of oil shale bearing deposits in the Hatıldağ oil shale field, Göynük, Turkey. *Fuel*, 1998, **77**(8), 871–880.
16. Hutton, A. C. Petrographic classification of oil shales. *Int. J. Coal Geol.*, 1987, **8**(3), 203–231.

17. Yıldırım, A., Şengüler, İ., Cihan, O. C., Hoşhan, P., Öner, A. *The organic and inorganic inventory and hydrocarbon potential of Türkiye oil shales*. Report No. 3864. Turkish Petroleum Corporation (TPAO) Research Center, 2014.
18. Peters, K. E. Guidelines for evaluating petroleum source rocks using programmed pyrolysis. *AAPG Bull.*, 1986, **70**, 318–329.
19. Abarghani, A., Ostadhassan, M., Gentzis, T., Carvajal-Ortiz, H., Bubach, B. Organofacies study of the Bakken source rock in North Dakota, USA, based on organic petrology and geochemistry. *Int. J. Coal Geol*., 2018, **188**, 79–93.
20. Abarghani, A., Ostadhassan, M., Gentzis, T., Carvajal-Ortiz, H., Bubach, B. Correlating Rock-Eval™ T_{max} with bitumen reflectance from organic petrology in the Bakken Formation. *Int. J. Coal Geol.*, 2019, **205**, 87–104.
21. Xiang-guo, L., Bao-guo, M., Li, X., Zhen-wu, H., Xin-gang, W. Thermogravimetric analysis of the co-combustion of the blends with high ash coal and waste tyres. *Thermochim. Acta*, 2006, **441**(1), 79–83.
22. Li, Q., Zhao, C., Chen, X., Wu, W., Li, Y. Comparison of pulverized coal combustion in air and in O_2/CO_2 mixtures by thermo-gravimetric analysis. *J. Anal. Appl. Pyrol.*, 2009, **85**(1–2), 521–528.
23. Qing, W., Chunxia, J., Qianqian, J., Yin, W., Wu, D. Combustion characteristics of Indonesian oil sands. *Fuel Proc. Technol.*, 2012, **99**, 110–114.
24. Tiwari, P., Deo, M. Compositional and kinetic analysis of oil shale pyrolysis using TGA–MS. *Fuel*, 2012, **94**, 333–341.
25. Thakur, D. S., Nuttall Jr., H. E. Kinetics of pyrolysis of Moroccan oil shale by thermogravimetry. *Ind. Eng. Chem. Res.*, 1987, **26**(7), 1351–1356.
26. Kissinger, H. E. Reaction kinetics in differential thermal analysis. *Anal. Chem*., 1957, **29**(11), 1702–1706.
27. Vyazovkin, S. Model-free kinetics. *J. Therm. Anal. Calorim.*, 2006, **83**, 45–51.
28. Al-Ayed, O. S., Matouq, M., Anbar, Z., Khaleel, A. M., Abu-Nameh, E. Oil shale pyrolysis kinetics and variable activation energy principle. *Applied Energy*, 2010, **87**(4), 1269–1272.
29. Syed, S., Qudaih, R., Talab, I., Janajreh, I. Kinetics of pyrolysis and combustion of oil shale sample from thermogravimetric data. *Fuel*, 2011, **90**(4), 1631–1637.
30. Torrente, M. C., Galán, M. A. Kinetics of the thermal decomposition of oil shale from Puertollano (Spain). *Fuel*, 2001, **80**(3), 327–334.
31. Aboulkas, A., El Harfi, K., Nadifiyine, M., Benchanaa, M. Pyrolysis behaviour and kinetics of Moroccan oil shale with polystyrene. *J. Petr. Gas Eng.*, 2011, **2**(6), 108–117.
32. Foltin, J. P., Prado, G. N., Lisbôa, A. C. L. Analysis of kinetics parameter of oil shale pyrolysis. *Chem. Eng. Trans.*, 2017, **61**, 439–444.
33. Hua, Z., Wang, Q., Jia, C., Liu, Q. Pyrolysis kinetics of a Wangqing oil shale using thermogravimetric analysis. *Energy Sci. Eng.*, 2019, **7**(3), 912–920.